ACS APPLIED MATERIALS & INTERFACES

Research Article

Cite This: ACS Appl. Mater. Interfaces 2019, 11, 17592−17601

www.acsami.org

Creation of Efficient Blue Aggregation-Induced Emission Luminogens for High-Performance Nondoped Blue OLEDs and Hybrid White OLEDs

Yinghao Li,[†,∥] Zeng Xu,[†,∥] Xiangyu Zhu,[†] Bin Chen,[†] Zhiming Wang,[†] Biao Xiao,[§] Jacky W. Y. Lam,[‡] Zujin Zhao,*[,†] Dongge Ma,*[,†] and Ben Zhong Tang[†,‡]

[†]State Key Laboratory of Luminescent Materials and Devices, Center for Aggregation-Induced Emission, South China University of Technology, Guangzhou 510640, China

[‡]Department of Chemistry, Hong Kong Branch of Chinese National Engineering Research Center for Tissue Restoration and Reconstruction, The Hong Kong University of Science and Technology, Clear Water Bay, Kowloon, Hong Kong 999077, China

[§]Key Laboratory of Optoelectronic Chemical Materials and Devices, Ministry of Education, School of Chemical and Environmental Engineering, Jianghan University, Wuhan 430056, China

Supporting Information

ABSTRACT: Organic blue luminescent materials are essential for organic light-emitting diodes (OLEDs). However, high-quality blue materials that can fulfill the requirements of OLED commercialization are much rare. Herein, two novel blue luminogens, 9-(4-(2,6-di-*tert*-butyl-10-(4-(1,2,2-triphenylvinyl)phenyl)anthracen-9-yl)phenyl)-9*H*-carbazole and 9-(4-(2,6-di-*tert*-butyl-10-(4-(1,2,2-triphenylvinyl)phenyl)anthracen-9-yl)1,3-di(9*H*-carbazol-9-yl)benzene (TPE-TADC), consisting of anthracene, tetraphenylethene, and carbazole groups are successfully prepared, and their thermal, optical, electronic, and electrochemical properties are fully investigated. They exhibit prominent aggregation-induced emission property and strong blue fluorescence at ∼455 nm in neat films. Efficient nondoped OLEDs are fabricated with these blue luminogens, providing blue electroluminescence (EL) at 451 nm ($CIE_{x,y}$ = 0.165, 0.141) and high EL efficiencies of 6.81 cd A^{-1}, 6.57 lm W^{-1}, and 5.71%. By utilizing TPE-TADC as a blue emissive layer, high-performance two-color hybrid white OLEDs are achieved, furnishing modulatable light color from pure white ($CIE_{x,y}$ = 0.33, 0.33) to warm white ($CIE_{x,y}$ = 0.44, 0.46) and excellent EL efficiencies of 56.7 cd A^{-1}, 55.2 lm W^{-1}, and 19.2%. More importantly, these blue and white OLEDs all display ultrahigh color and efficiency stabilities at high luminance, indicating the great potential of these blue luminogens for the application in OLED displays and white illumination.

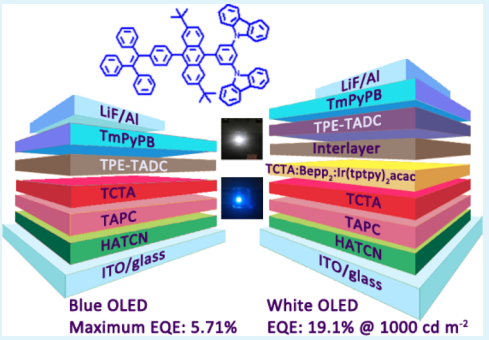

KEYWORDS: *aggregation-induced emission, blue emitter, tetraphenylethene, anthracene, white OLED*

1. INTRODUCTION

Organic light-emitting diodes (OLEDs) have drawn persistent interest and advanced rapidly, owing to their outstanding merits of self-emitting nature, flexible display potential, low-energy consumption, and fast response.[1−3] Despite many successes have been achieved in some commercial OLED products in this area, thorny obstacles still exist in realizing large-scale applications. For example, the performance of blue OLEDs is actually not good enough, in terms of efficiency and stability,[4] which are significantly dependent on the blue luminescent materials. The noble-metal-containing phosphorescent blue emitters often encounter stability problem, whereas the purely organic luminescent materials with thermally activated delayed fluorescence can only give sky blue emission in most cases because of the strong charge-transfer nature. In addition, the blue emitters intrinsically require wide energy band gaps, which make the carrier injection difficult in turn.[5−9] In consequence, high-quality blue emitters are highly insufficient and the exploration of robust blue emitters remains a challenging task.

Anthracene has good photoluminescence (PL) and carrier-transporting ability and is the first chromophore applied to electroluminescence (EL) investigation.[10−15] However, its planar and rigid structure makes it easy to experience strong $\pi-\pi$ interaction in the aggregated state, which weakens or seriously quenches fluorescence. In consequence, many blue emitters of anthracene derivatives show decreased emissions in neat films and have to be doped into wide band gap hosts for the application of OLEDs. Although the doping technology solves the problem to some extent, it also complicates the

Received: February 20, 2019
Accepted: April 23, 2019
Published: April 23, 2019

DOI: 10.1021/acsami.9b03177
ACS Appl. Mater. Interfaces 2019, 11, 17592−17601

Scheme 1. Synthetic Routes towards New Blue AIEgens, TPE-TAC, and TPE-TADC

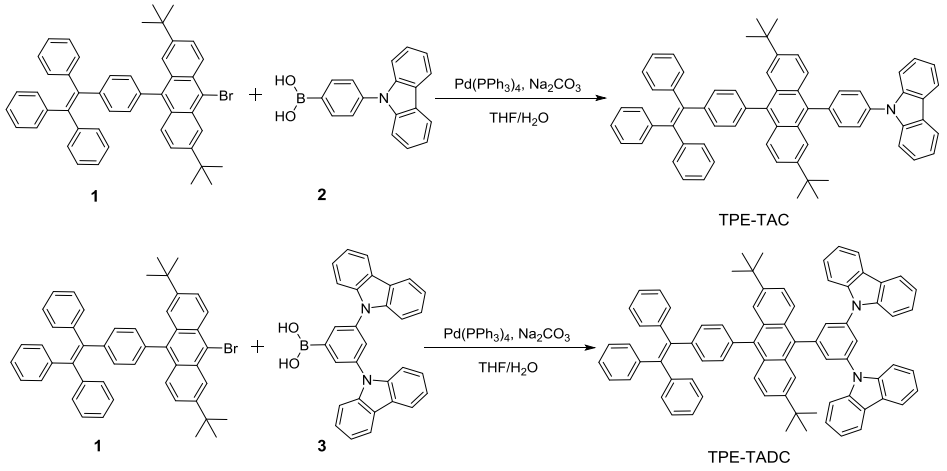

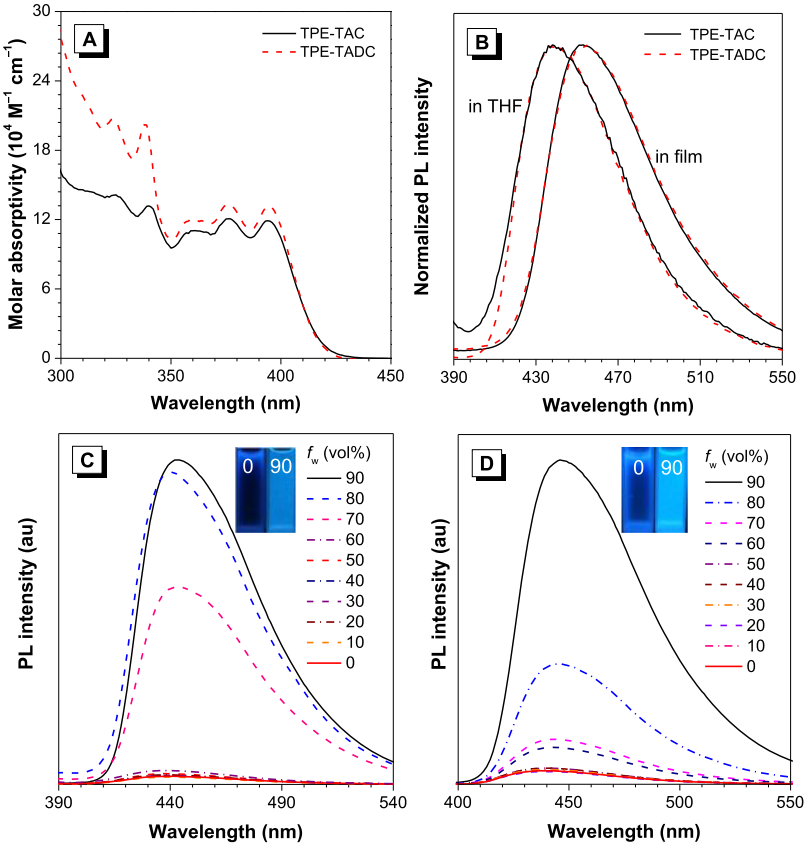

Figure 1. (A) Absorption spectra of TPE-TAC and TPE-TADC in THF solutions (10 μM). (B) PL spectra of TPE-TAC and TPE-TADC in THF solutions and solid films. PL spectra of (C) TPE-TAC and (D) TPE-TADC in THF/water mixtures at different water fractions (f_w).

device structure, increases the cost, and reduces the reproducibility.[16−20] To address this issue, a strategy of molecularly melding aggregation-induced emission (AIE) moieties, such as tetraphenylethene (TPE), with conventional chromophores is proposed, which has generated various luminescent materials with fluorescence color covering the entire visible light region.[21−23] These TPE-functionalized emitters are free of aggregation-caused quenching and can emit strong fluorescence in neat films,[24] which enable them to function efficiently in nondoped OLEDs.

In this work, we wish to report two efficient blue luminogens from anthracene derivatives, TPE-TAC and TPE-TADC, for the use in nondoped OLEDs. In these luminogens, AIE-active TPE is attached to an anthracene core modified with branched *tert*-butyl groups to impede strong intermolecular interactions and improve emission efficiency in the aggregated state. Moreover, carbazole groups are introduced to increase carrier transport as well as triplet energy levels. The results reveal that TPE-TAC and TPE-TADC exhibit excellent AIE characteristics with blue PL peaks at 452 nm and high fluorescence quantum yields (Φ_{FS}) over 70% in neat films. Notably, their nondoped OLEDs display blue EL at 451 nm and high EL efficiencies (5.11 and 5.71%). In addition, high-performance two-color hybrid white OLEDs are achieved based on TPE-

DOI: 10.1021/acsami.9b03177
ACS Appl. Mater. Interfaces 2019, 11, 17592−17601

Table 1. Photophysical Properties, Thermal Stabilities, and Energy Levels of the New Blue AIEgens

		λ_{em} (nm)		Φ_F (%)[b]				τ (ns)		
	λ_{abs} (nm)	THF	film[a]	THF	film[a]	α_{AIE}[c]	HOMO/LUMO/E_g (eV)[d]	THF	film[a]	T_g/T_d (°C)
TPE-TAC	394	438	453	2.1	76.7	36.5	−5.32/−2.57/2.75	1.96	2.99	165/429
TPE-TADC	395	440	455	2.5	72.8	29.1	−5.37/−2.55/2.82	2.16	3.20	−/486

[a]Solid neat film. [b]Absolute fluorescence quantum yield determined by a calibrated integrating sphere. [c]The value of AIE effect reckoned as Φ_F (film)/Φ_F (THF). [d]Determined by CV.

TADC, furnishing excellent EL efficiencies (56.7 cd A^{-1}, 55.2 lm W^{-1}, and 19.2%), ultrahigh color stability, and low efficiency roll-off.

2. RESULTS AND DISCUSSION

2.1. Synthesis. Scheme 1 displays synthetic routes toward these two new blue luminogens, TPE-TAC and TPE-TADC. Compounds **1**−**3** are prepared by the reported methods.[25,26] TPE-TAC and TPE-TADC are synthesized by Suzuki couplings of **1** with **2** and **3**, respectively, in high yields. All of the final products are fully characterized by NMR and mass spectroscopies. Detailed procedures and characterization data are described in the Supporting Information. Both TPE-TAC and TPE-TADC have good solubility in dichloromethane, chloroform, tetrahydrofuran (THF), and toluene, but poor solubility in water.

2.2. Photophysical Properties. TPE-TAC and TPE-TADC show intense absorption maxima at ∼395 nm (Figure 1A) in dilute THF solution (10 μM), ascribed to the $\pi-\pi^*$ transition of the planar anthracene core. TPE-TAC and TPE-TADC display weak blue PL peaks located at 438 and 440 nm with poor Φ_Fs of merely 2.1 and 2.5% (Table 1), respectively, indicating that they are faint emitters in the solution state. These poor PL behaviors are widely observed for many TPE derivatives[27−31] because the intramolecular rotation of TPE moieties can result in the nonradiative relaxation of excited state and quench emission. On the contrary, TPE-TAC and TPE-TADC become highly emissive in solid films with strong PL peaks located at 453 and 455 nm and high Φ_Fs of 76.7 and 72.8%, respectively. In addition, the fluorescence lifetimes (τ) are measured to be 2.99 and 3.20 ns in films, much longer than those in dilute THF (1.96 and 2.16 ns), which are consistent with their Φ_Fs in films and solutions. These results disclose that they are AIE-active. To further validate their AIE properties, the PL behaviors in THF/water mixtures are measured (Figure 1B). It is observed that as the water content gets higher than 70%, the PL intensity of TPE-TAC is enhanced notably. Similar PL enhancement can also be found for TPE-TADC. Because both molecules are insoluble in water, they must form aggregates when the water content gets high. Thus, the PL is induced by aggregate formation, demonstrating the AIE behaviors. In aggregates, the intramolecular rotation is restricted by spatial constraint. Therefore, the nonradiative decay channel is blocked, and the excited state is relaxed in a radiative manner, leading to strong PL.

2.3. Theoretical Calculation. To study the electronic structures, time-dependent density functional theory calculation with a B3LYP/6-31G (d) basis set is carried out on TPE-TAC and TPE-TADC.[32] Their optimized structures show that they prefer to adopt highly twisted conformations, in which carbazole and TPE moieties are twisted out of the anthracene plane. In addition, very large torsion angles in the range of 76.54°−103.46° are found between the anthracene core and 9,10-positioned phenyl rings (Figure 2). Such twisted

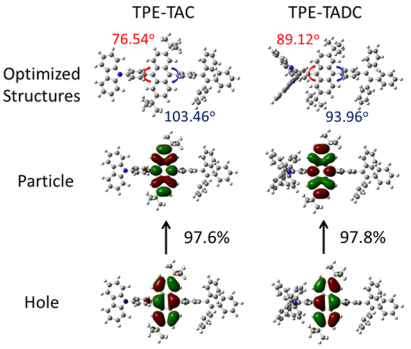

Figure 2. Natural transition orbital analysis for the S_1 states based on ground state optimized structures of TPE-TAC and TPE-TADC, calculated by B3LYP/6-31G (d) basis set. The predominant wave functions of hole and particle with the largest weight are illustrated.

conformations as well as the presence of *tert*-butyl groups can efficiently prevent molecules from close stacking, which suppresses strong intermolecular interactions and thus ensures efficient emission in the aggregated state. The transitions of the ground states (S_0) to the lowest singlet excited states (S_1) of both luminogens are highly associated with the transitions from the highest occupied molecular orbitals (HOMOs) to the lowest unoccupied molecular orbitals (LUMOs). The wave functions of both HOMOs and LUMOs are majorly distributed on the anthracene core, and other moieties show little contribution. The energy levels of HOMOs and LUMOs are calculated to be −5.00 and −1.66 eV for TPE-TAC, and −5.05 and −1.73 eV for TPE-TADC, respectively.

2.4. Electrochemical Behaviors. To investigate the electrochemical properties, TPE-TAC and TPE-TADC are subjected to the cyclic voltammetry (CV) measurement (Figure 3). Both luminogens show reversible oxidation and reduction processes, implying that they are electrochemically stable. On the basis of the equation [HOMO = −(E_{ox} + 4.8 − $E_{ox,fc}$) eV], in which E_{ox} is the onset oxidation potential of the luminogens, 4.8 eV is the assumed absolute energy level of F_c/F_{c+} below vacuum, and $E_{ox,fc}$ is the onset oxidation potential of F_c/F_{c+},[33,34] HOMO energy levels of TPE-TAC and TPE-TADC are determined to be −5.32 and −5.37 eV, respectively. The HOMO energy levels of TPE-TAC and TPE-TADC are approximate to those of popular hole-transporting materials, such as 1,1-bis[(di-4-tolylamino)phenyl]cyclohexane (TAPC, −5.3 eV),[37] implying that the hole injection and transport are favorable in both luminogens. The LUMO energy levels can be obtained through the calculation of [LUMO = −(E_{re} + 4.8 − $E_{re,fc}$) eV], where E_{re} is the onset reduction potential of the luminogens and $E_{re,fc}$ is the onset reduction potential of F_c/F_{c+}.[32,34] Therefore, the LUMO energy levels of TPE-TAC and TPE-TADC can be obtained as −2.57 and −2.54 eV, respectively, being close to that of 1,3,5-tri(*m*-pyrid-3-yl-phenyl)benzene (TmPyPB, −2.7 eV).[38]

DOI: 10.1021/acsami.9b03177
ACS Appl. Mater. Interfaces 2019, 11, 17592−17601

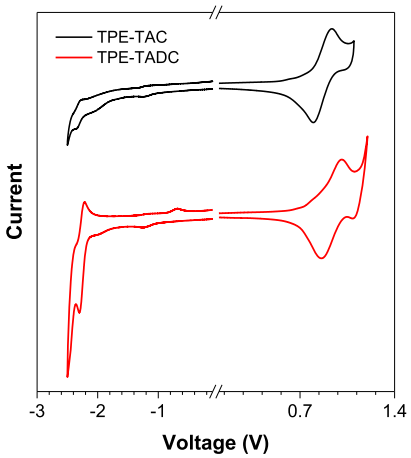

Figure 3. Cyclic voltammograms of TPE-TAC and TPE-TADC, measured in *N*,*N*-dimethylformamide (negative) and in dichloromethane (positive) containing tetra-*n*-butylammonium hexafluorophosphate (0.1 M) at a scan rate of 50 mV s^{-1}.

2.5. Thermal Stability. Generally, to fabricate high-performance OLEDs, good thermal stability of the emitters is important, especially in the vacuum deposition process. Hence, the thermal properties of TPE-TAC and TPE-TADC are investigated by thermogravimetric analysis (TGA) and differential scanning calorimetry (DSC) under nitrogen. As depicted in Figure 4, TPE-TAC and TPE-TADC show high thermal decomposition temperatures (T_d) at 429 and 486 °C, respectively, corresponding to 5% loss of the initial weight. In addition, TPE-TAC shows a high glass-transition temperature (T_g) of 165 °C, indicating the excellent morphological stability. No T_g is observed for TPE-TADC. These thermal tests demonstrate that TPE-TAC and TPE-TADC are thermally stable, which is favored to fabricate stable OLEDs.

2.6. Nondoped Blue OLEDs. The application of TPE-TAC and TPE-TADC as light-emitting layers is evaluated in nondoped OLEDs with a configuration of ITO/1,4,5,8,9,11-hexaazatriphenylenehexacarbonitrile (HATCN) (5 nm)/TAPC (50 nm)/tris(4-carbazoyl-9-ylphenyl)amine (TCTA) (5 nm)/emitter (20 nm)/bis[2-(2-hydroxyphenyl)-pyridine] beryllium ($Bepp_2$) (40 nm)/LiF (1 nm)/Al, in which the emitter is TPE-TAC or TPE-TADC, and HATCN, TAPC, TCTA, and $Bepp_2$ are employed as hole injection, hole-transporting, exciton-blocking, and electron-transporting layers, respectively.[35−38] The device fabrication and measurement are carried out according to the reported methods.[25] The devices utilizing TPE-TAC and TPE-TADC as emitters radiate blue light at 452 and 451 nm with Commission Internationale de L'Eclairage ($CIE_{x,y}$) of (0.161, 0.135) and (0.164, 0.140), respectively, which is almost identical to their PL in solid films, indicating that singlet excitons are directly recombined within light-emitting layers for the blue light emission. The device of TPE-TAC displays good EL performance of a maximum luminance (L_{max}) of 6382 cd m^{-2}, a maximum current efficiency ($\eta_{C,max}$) of 5.86 cd m^{-2}, a maximum power efficiency ($\eta_{P,max}$) of 5.55 lm W^{-1}, and a maximum external quantum efficiency ($\eta_{ext,max}$) of 4.79 (Table 2). In comparison with TPE-TAC, the TPE-TADC-based device exhibits even better EL performance of a L_{max} of 7397 cd m^{-2}, a $\eta_{C,max}$ of 6.18 cd m^{-2}, a $\eta_{P,max}$ of 6.05 lm W^{-1}, and a $\eta_{ext,max}$ of 5.06%. The performances of these devices have surpassed many of the conventional blue fluorescent OLEDs.

To further improve the EL performances, the device configuration is optimized by adopting different electron-transporting layers with different energy levels. 1,3-Bis(3,5-dipyrid-3-yl-phenyl)benzene (BmPyPB), TmPyPB, and 4,7-diphenyl-1,10-phenanthroline (Bphen) are introduced as electron-transporting and hole-blocking layers to replace $Bepp_2$. These new devices fabricated from TPE-TAC and TPE-TADC also exhibit excellent EL performances (Table 2 and Figure 5). They can be turned on at low voltages of 2.9−3.3 eV and exhibit blue EL peaks at 451−455 nm, which are actually barely changed in comparison with the previous devices. Amongst them, the devices constructed with TmPyPB that possesses the lowest HOMO (−6.7 eV) and highest electron mobility of 1.0×10^{-3} cm^2 V^{-1} s^{-1} afford the better EL efficiencies of 6.19 cd A^{-1} ($\eta_{P,max}$), 5.81 lm W^{-1} ($\eta_{P,max}$), and 5.11% ($\eta_{ext,max}$) for TPE-TAC and 6.81 cd A^{-1} ($\eta_{P,max}$), 6.57 lm W^{-1} ($\eta_{P,max}$), and 5.71% ($\eta_{ext,max}$) for TPE-TADC, which are close to the theoretical limits of conventional fluorescent OLEDs. Concerning that the LUMO energy level of $Bepp_2$ (−5.7 eV) is only slightly lower than those of TPE-TAC and TPE-TADC, its hole-blocking ability may be not good enough for these devices. Therefore, the resulting improvement in EL efficiencies could be attributed to that TmPyPB prevents leakage current and balances the carrier transport of the devices (Figure 6).

2.7. Carrier Transport. To better elucidate the excellent EL performances, the carrier mobility of TPE-TAC and TPE-TADC is evaluated by the space-limited current (SCLC) method. They are applied to electron- and hole-only devices

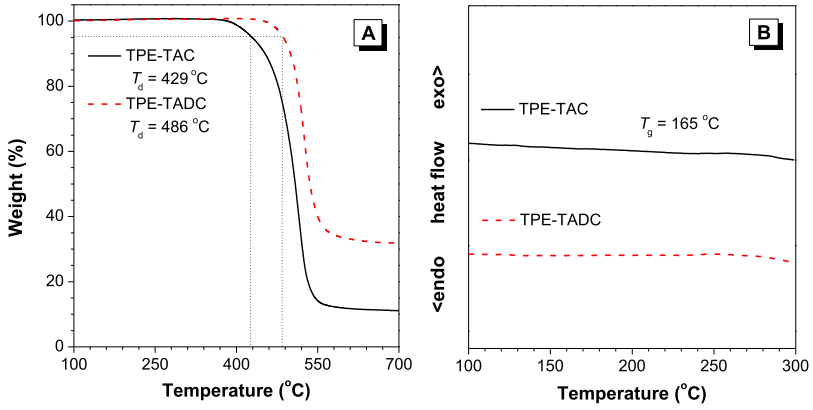

Figure 4. (A) TGA and (B) DSC curves of TPE-TAC and TPE-TADC recorded in nitrogen atmosphere (heating rate: 10 °C min^{-1}).

DOI: 10.1021/acsami.9b03177
ACS Appl. Mater. Interfaces 2019, 11, 17592−17601

Table 2. Performance Data of Blue OLEDs of TPE-TAC and TPE-TADC

ETL[a]	V_{on} (V)	L_{max} (cd m^{-2})	$\eta_{C,max}$ [b] (cd A^{-1})	$\eta_{P,max}$ [b] (lm W^{-1})	$\eta_{ext,max}$ [b] (%)	λ_{max} (nm)	CIE$_{(x,y)}$
ITO/HATCN (5 nm)/TAPC (50 nm)/TCTA (5 nm)/TPE-TAC (20 nm)/ETL (40 nm)/LiF (1 nm)/Al							
BmPyPB	3.1	1890	6.06/3.83	5.35/1.84	5.04/3.34	455	(0.156, 0.136)
TmPyPB	3.1	3898	6.19/4.29	5.81/2.32	5.11/3.89	452	(0.159, 0.127)
Bepp$_2$	3.0	6382	5.86/3.75	5.55/2.14	4.79/3.25	452	(0.161, 0.135)
Bphen	3.1	3469	5.16/3.21	4.88/1.84	4.45/2.76	452	(0.162, 0.138)
ITO/HATCN (5 nm)/TAPC (50 nm)/TCTA (5 nm)/TPE-TADC (20 nm)/ETL (40 nm)/LiF (1 nm)/Al							
BmPyPB	3.3	2593	6.39/4.62	5.54/2.58	5.37/3.96	453	(0.158, 0.137)
TmPyPB	3.0	4036	6.81/5.13	6.57/3.36	5.71/4.41	451	(0.165, 0.141)
Bepp$_2$	2.9	7397	6.18/4.47	6.05/2.87	5.06/3.75	452	(0.164, 0.140)
Bphen	2.9	4540	6.15/4.66	6.02/3.10	5.23/4.02	452	(0.162, 0.135)

[a]Abbreviation: ETL = electron-transporting layer, λ_{EL} = EL peak at 1000 cd m^{-2}, V_{on} = turn-on voltage at 1 cd m^{-2}, L_{max} = maximum luminance, $\eta_{C,max}$ = maximum current efficiency, $\eta_{P,max}$ = maximum current efficiency, $\eta_{ext,max}$ = maximum external quantum efficiency, CIE = Commission Internationale de l'Eclairage coordinates at 1000 cd m^{-2}. [b]Order of maximum and the value at 1000 cd m^{-2}.

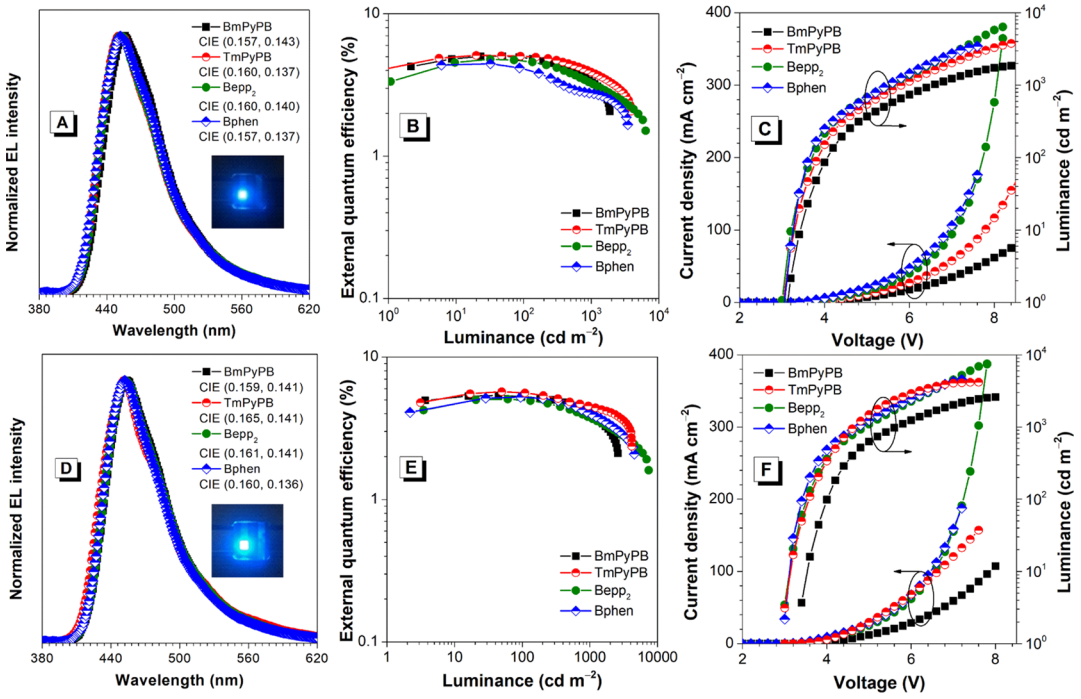

Figure 5. (A,D) EL spectra, (B,E) external quantum efficiency–luminance curves, and (C,F) current density–voltage–luminance plots of the nondoped blue OLEDs.

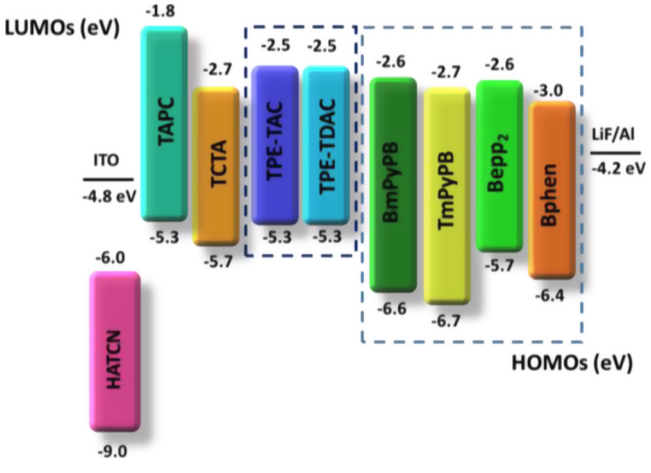

Figure 6. Energy level diagrams of nondoped blue OLEDs based on TPE-TAC and TPE-TDAC.

with configurations of ITO/TmPyPB (10 nm)/TPE-TAC or TPE-TADC (80 nm)/LiF (1 nm)/Al and ITO/TPE-TAC or TPE-TADC (80 nm)/TAPC (10 nm)/Al, respectively. The carrier mobility (μ) can be calculated by the Poole–Frenkel eq 1

$$\mu = \mu_0 \exp(\gamma\sqrt{E}) \quad (1)$$

in which γ, the Poole–Frenkel factor, and μ_0, the zero-field mobility, are expressed from fitting the current density–voltage curves in the SCLC region (Figure 7). At an electric field of 5.5 × 10^5 V cm^{-1}, generally corresponding to 1000 cd m^{-2}, the electron mobilities of TPE-TAC and TPE-TADC are determined to be 1.21 × 10^{-6} and 1.47 × 10^{-6} cm^2 V^{-1} s^{-1}, whereas the hole mobilities are 5.49 × 10^{-6} and 7.96 × 10^{-6} cm^2 V^{-1} s^{-1}, respectively, under the same condition. Clearly, both new luminogens exhibit better hole transport than electron transport owing to the introduction of carbazole moiety. Therefore, the use of TmPyPB with good hole-blocking and electron-transporting abilities can indeed balance

DOI: 10.1021/acsami.9b03177
ACS Appl. Mater. Interfaces 2019, 11, 17592–17601

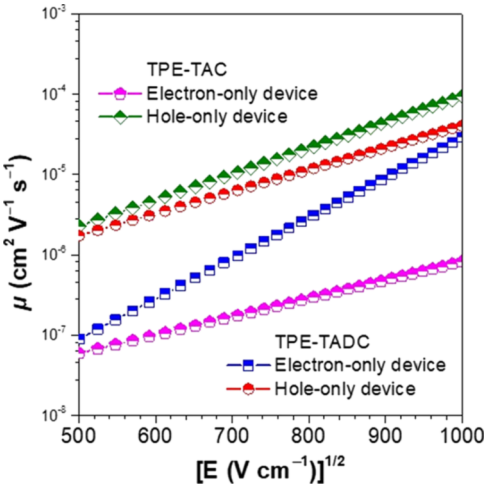

Figure 7. Electric field-dependent hole and electron mobilities (μ) of TPE-TAC and TPE-TADC.

carrier transport and eventually increase the EL efficiencies of the OLEDs based on TPE-TAC and TPE-TADC.

2.8. Light Out-Coupling Efficiency. To gain a high EL efficiency, the light out-coupling efficiency is another very important factor, in addition to the PL efficiency, exciton utilization, and carrier recombination. For a neat film of common organic molecule, the light out-coupling efficiency generally falls in the range of 0.2−0.3. However, the regular horizontal orientation of transition dipole moment of the molecule can effectively improve the light out-coupling efficiency (>0.3) and thus increase EL efficiency, which is considered as a main cause for the abnormally high EL efficiencies of certain emitters.[39] In view of this, we envision that the horizontal orientation may exist in the neat film of TPE-TADC. The measurement of horizontal orientation generally requires angle-resolved and polarization-resolved PL spectra.[40] However, we currently do not have such kind of instruments to conduct this measurement. Therefore, we use another method, variable angle spectroscopic ellipsometry (VASE), to evaluate the horizontal orientation by investigating the anisotropy of the neat film of TPE-TADC.[41] VASE was reported to be able to evaluate the degree of molecular and dipole orientations in neat organic thin films. An orientation order parameter S is defined to quantify the orientation of the dipole moment, as the following eq 2

$$S = \frac{k_z^{max} - k_x^{max}}{k_z^{max} + 2k_x^{max}} \quad (2)$$

in which k_x^{max} and k_z^{max} are the peak ordinary and extraordinary extinction coefficients attributed to the transition dipole moment, respectively. When $-0.5 < S < 0$, the molecules are horizontally oriented in some extent. As depicted in Figure 8, the k_x^{max} is higher than k_z^{max}. As a result, the S value is calculated to be −0.133, revealing the preferential horizontal orientation of the TPE-TADC's transition dipole moment. Conclusively, the light out-coupling efficiency of the TPE-TADC film could be larger than 0.3, which contributes to the excellent $\eta_{ext,max}$ of the nondoped OLED of TPE-TADC.

2.9. Hybrid White OLEDs. The excellent EL performances of nondoped blue OLEDs of TPE-TAC and TPE-TADC prompt us to investigate their potentials for the application in white OLEDs.[42−44] Encouraged by the high EL efficiencies of

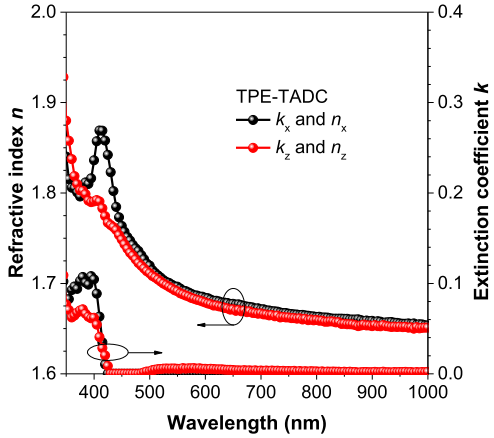

Figure 8. Anisotropy in extinction coefficients and refractive indices of the TPE-TADC film (40 nm) deposited on the silicon substrate.

TPE-TADC, we introduce an efficient yellow phosphor, iridium(III) bis(4-(4-*tert*-butylphenyl) thieno[3,2-*c*]-pyridinato-*N*,C2′) acetylacetonate (It(tptpy)$_2$acac), into the optimal nondoped device with a TmPyPB electron-transporting layer to construct two-color hybrid white OLEDs.[45−47] To block energy transfer between TPE-TADC and It(tptpy)$_2$acac, a bipolar interlayer (3 nm) composed of electron-transporting Bepp$_2$ and hole-transporting TCTA is added between these two luminescent materials to regulate the diffusions of carriers and excitons. The reason why Bepp$_2$ and TCTA are selected is that they possess moderate HOMO and LUMO energy levels and high triplet energy levels of 2.60 and 2.76 eV, respectively, which can not only prevent the quenching of triplet excitons in It(tptpy)$_2$acac but also ensure high carrier-transporting ability.[48−50] In addition, It(tptpy)$_2$acac is doped in the TCTA and Bepp$_2$ mixture with a weight ratio of 0.40:0.57:0.03 to reduce the concentration quenching. On the basis of above considerations, we have developed hybrid white OLEDs with a configuration of ITO/HATCN (5 nm)/TAPC (50 nm)/TCTA (5 nm)/TCTA−Bepp$_2$−Ir(tptpy)$_2$acac (0.40:0.57:0.03, 15 nm)/interlayer (Bepp$_2$−TCTA) (3 nm)/TPE-TADC (10 nm)/TmPyPB (40 nm)/LiF (1 nm)/Al, where TAPC and TCTA act as stepwise hole-transporting layers, and Bepp$_2$ and TmPyPB as electron-transporting layers (Figure 9).

By optimizing the co-doping weight ratio of the interlayer Bepp$_2$−TCTA to 3:2, a high-performance white OLED (W3) is obtained. As shown in Table 2, the device W3 gives excellent $\eta_{C,max}$, $\eta_{P,max}$, and $\eta_{ext,max}$ of 56.7 cd A^{-1}, 55.2 lm W^{-1}, and 19.2%, respectively, being comparable to those of the most efficient hybrid white OLEDs. Considering that the out-

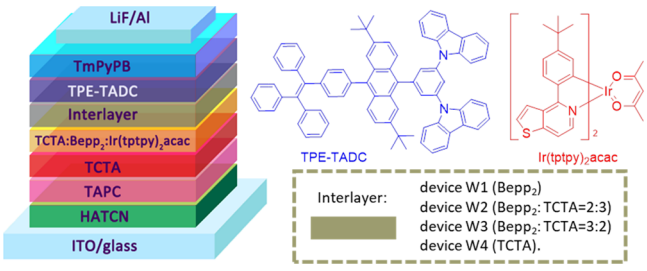

Figure 9. Schematic configuration of two-color hybrid white OLED and the chemical structures of the two emitters.

DOI: 10.1021/acsami.9b03177
ACS Appl. Mater. Interfaces 2019, 11, 17592−17601

coupling efficiency of common OLEDs is generally 20%, the internal quantum efficiency has already reached nearly 100%.[51−53] In addition, this device displays ultrahigh color and efficiency stability. As shown in Figure 10, the EL peaks at

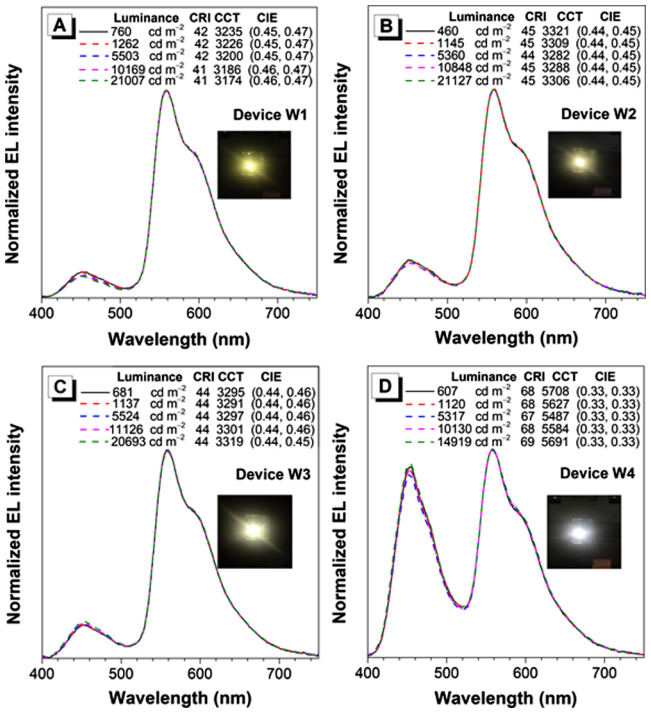

Figure 10. (A−D) EL spectra of the white OLEDs at varied luminance. Configuration: ITO/HATCN (5 nm)/TAPC (50 nm)/TCTA (5 nm)/TCTA−$Bepp_2$−$Ir(tptpy)_2acac$ (0.40:0.57:0.03, 15 nm)/interlayer (3 nm)/TPE-TADC (10 nm)/TmPyPB (40 nm)/LiF (1 nm)/Al. Interlayer: $Bepp_2$ (device W1), $Bepp_2$−TCTA = 2:3 (device W2), $Bepp_2$−TCTA = 3:2 (device W3), and TCTA (device W4).

452 and 558 nm are apparently derived from TPE-TADC and $Ir(tptpy)_2acac$, respectively. The EL spectral profiles are almost unchanged as luminance increases. Even at a high luminance of 20 000 cd m^{-2}, the color correlated temperature (CCT) span still maintains a low color temperature of ∼3300, with a variation less than 40, corresponding to a satisfactory constant $CIE_{x,y}$ of (0.44, 0.46), which is rarely reported in white OLEDs.[54−60] Moreover, device W3 shows a η_C of 56.5 cd A^{-1} and a η_{ext} of 19.1% at 1000 cd m^{-2}. In addition, at 5000 cd m^{-2}, the η_C and η_{ext} still remain as 52.5 cd A^{-1} and 17.8%, respectively, demonstrating remarkable efficiency stability.

The device W2 with an interlayer of $Bepp_2$−TCTA (2:3) also shows good EL efficiencies of 53.4 cd A^{-1}, 42.8 lm W^{-1}, and 18.4% at 1000 cd m^{-2} and maintains high values of 51.3 cd A^{-1} and 17.6% at 5000 cd m^{-2}, indicating the good efficiency stability. However, compared with device W3, the performances of device W2 are slightly inferior. This may be ascribed to the higher doping ratio of $Bepp_2$ in the interlayer of device W3. With an increased ratio of electron-transporting $Bepp_2$, device W3 can ensure the triplet excitons diffusing from blue fluorescent TPE-TADC to yellow phosphorescent $Ir(tptpy)_2acac$, achieving the full utilization of excitons, which is consistent with the device results. Besides, TCTA has a higher triplet energy level (2.76 eV) than the adjacent $Bepp_2$ (2.6 eV) host, indicating that TCTA has a better ability to confine triplet excitons within the yellow phosphorescent $Ir(tptpy)_2acac$ layer. In other words, triplet excitons are more difficult to escape from the yellow $Ir(tptpy)_2acac$ layer in white OLEDs with a co-doping interlayer of TCTA and $Bepp_2$ than a sole interlayer of $Bepp_2$. Consequently, the EL efficiencies of device W1 (with maxima values of 49.2 cd A^{-1}, 46.8 lm W^{-1}, and 16.3%) are lower relative to those of devices W2 and W3 as its interlayer is completely composed of $Bepp_2$.

To further verify the influence of interlayer, device W4 with an interlayer of TCTA is fabricated and investigated. Owing to the absence of $Bepp_2$, much less triplet excitons are harnessed by $It(tptpy)_2acac$ via triplet exciton diffusion mechanism, which means device W4 may exhibit a poor performance and lead to a movement of exciton recombination region from yellow layer to blue layer. To get evidences for the above analyses, the EL spectra of device W4 at varied luminance are measured. Overall, the blue EL intensity is greatly increased, whereas the yellow EL intensity is decreased, disclosing that more excitons are generated in the blue TPE-TADC layer and less triplet excitons can overcome the barrier of interlayer to arrive at the yellow $It(tptpy)_2acac$ layer. Therefore, triplet excitons in blue TPE-TADC may be quenched through nonradiative relaxation, causing a decrease in EL efficiency. Indeed, the EL efficiencies of device W4 are merely 24.2 cd A^{-1}, 21.3 lm W^{-1}, and 10.3%, almost half of those of device W3, which confirms our previous analyses. One thing should be mentioned is that via such kind of exciton diffusion modulation, device W4 has successfully achieved a pure white light with $CIE_{x,y}$ coordinate of (0.33, 0.33) over a broad luminance range of 144−14 919 cd m^{-2} and a moderate color rendering index (CRI) of 68 (Table 3).

Generally, most of the reported high-performance white OLEDs are fabricated based on a complicated configuration with multiple light-emitting layers. Under high-driven voltages, the exciton recombination region tends to transfer, which will

Table 3. Performance Data of Hybrid White OLEDs Based on TPE-TADC

device	V_{on} (V)	L_{max} (cd m^{-2})	η_C[a] (cd A^{-1})	η_P[a] (lm W^{-1})	η_{ext}[a] (%)	CRI[b]	CCT[b]	$CIE_{(x,y)}$[b]
W1	2.8	57 489	49.2/49.1/48.0	46.8/41.7/31.0	16.3/16.3/15.9	42	3226	(0.45, 0.47)
W2	2.8	54 829	53.5/53.4/51.3	49.9/42.8/28.3	18.4/18.4/17.6	45	3309	(0.44, 0.45)
W3	2.8	49 002	56.7/56.5/52.5	55.2/47.5/32.7	19.2/19.1/17.8	44	3291	(0.44, 0.46)
W4	3.0	17 064	24.2/23.9/21.7	21.3/16.1/9.6	10.3/10.2/9.2	68	5627	(0.33, 0.33)

[a]Order of maximum, then values at 1000, and 5000 cd m^{-2}. [b]Measured at 1000 cd m^{-2}, CRI = color rendering indexes, CCT = color correlated temperature (CCT) span, CIE = Commission Internationale de l'Eclairage coordinates at 1000 cd m^{-2}. Device configuration: ITO/HATCN (5 nm)/TAPC (50 nm)/TCTA (5 nm)/TCTA−$Bepp_2$−$Ir(tptpy)_2acac$ (0.40:0.57:0.03, 15 nm)/interlayer (3 nm)/TPE-TADC (10 nm)/TmPyPB (40 nm)/LiF (1 nm)/Al. Interlayer: $Bepp_2$ (device W1), $Bepp_2$−TCTA = 2:3 (device W2), $Bepp_2$−TCTA = 3:2 (device W3), and TCTA (device W4).

DOI: 10.1021/acsami.9b03177
ACS Appl. Mater. Interfaces 2019, 11, 17592−17601

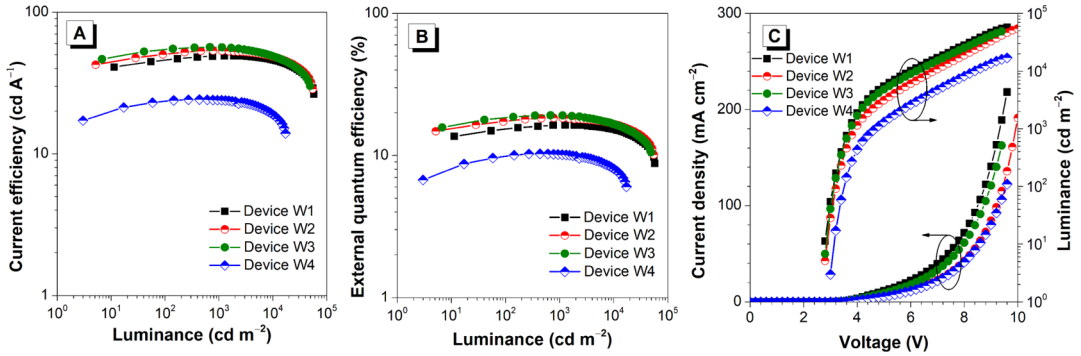

Figure 11. Plots of (A) current efficiency–luminance, (B) external quantum efficiency–luminance, and (C) current density–voltage–luminance of the white OLEDs.

result in an enhanced blue EL intensity, namely, poor color stability. Even worse, although high EL efficiencies have been reported in many literatures, most of them are only achieved at low luminance and suffer from severe roll-off when the luminance reaches 3000–5000 cd m^{-2} or higher. It is worth noting that excellent efficiency stability has been achieved in these devices and all of the four white OLEDs exhibit very small external quantum efficiency roll-off less than 10% at high luminance of 5000 cd m^{-2} (Figure 11). In addition, almost no changes in CRI, CIE coordinate, and EL spectra are observed over a broad luminance range of 500–20 000 cd m^{-2}, which are comparable to the commercial lighting devices such as Xe Lamp lamps or LEDs. The reduced efficiency roll-off and improved color stability are attributed to the wide exciton recombination region and bipolar charge transport ability of the interlayer. Moreover, the turn-on voltages of these white OLEDs (W1–W3) are as low as ~2.8 eV, indicating the balanced carrier transport and injection. In a word, by adjusting the interlayer, these white OLEDs not only give high performance but also display excellent efficiency and color stability at high luminance, demonstrating the great commercialization potential of both new blue luminogens.

3. CONCLUSIONS

In this contribution, two robust blue luminogens TPE-TAC and TPE-TADC composed of a *tert*-butyl modified anthracene core and TPE and carbazole functional substituents are successfully synthesized and thoroughly investigated. They hold good thermal and electrochemical stabilities and exhibit prominent AIE property with PL peaks at 453 and 455 nm and excellent Φ_Fs of 76.7 and 72.8% in neat films, respectively. Efficient nondoped OLEDs are fabricated based on these blue luminogens, affording blue EL at 451 nm (CIE$_{x,y}$ = 0.165, 0.141) and high EL efficiencies of up to 5.71%, approaching theoretical limit of common fluorescent OLEDs. Moreover, high-performance hybrid white OLEDs adopting TPE-TADC neat film as a blue-emitting layer and It(tptpy)$_2$acac doped film as a yellow-emitting layer are achieved. They have low turn-on voltages at 2.8–3.0 V and exhibit excellent EL efficiencies of 56.7 cd A^{-1}, 55.2 lm W^{-1}, and 19.2%. By optimizing the interlayer between blue- and yellow-emitting layers, a white OLED with pure white color (CIE$_{x,y}$ = 0.33, 0.33) is obtained. Moreover, these blue and white OLEDs display ultrahigh color stability and low efficiency roll-off at high luminance, demonstrating important features of OLEDs based on AIEgens. These efficient luminogens show comparable EL efficiencies to previously reported AIEgens but have bluer EL emissions.[25] Their increased light out-coupling efficiency, balanced carrier transport, and suitable energy levels make contributions to the excellent EL performances. They can provide a competitive advantage in displays and lighting applications based on the OLED technique.

■ ASSOCIATED CONTENT

Supporting Information

The Supporting Information is available free of charge on the ACS Publications website at DOI: 10.1021/acsami.9b03177.

General information, synthetical procedures and characterization data, device fabrication and measurement, carrier transport calculation, fluorescence decay profiles, chemical structures of active layers, and NMR spectra (PDF)

■ AUTHOR INFORMATION

Corresponding Authors

*E-mail: mszjzhao@scut.edu.cn (Z.Z.).
*E-mail: msdgma@scut.edu.cn (D.M.).

ORCID

Zhiming Wang: 0000-0002-3047-3285
Zujin Zhao: 0000-0002-0618-6024
Ben Zhong Tang: 0000-0002-0293-964X

Author Contributions

‖These authorsY.L. and Z.X. contributed equally to the work.

Notes

The authors declare no competing financial interest.

■ ACKNOWLEDGMENTS

We acknowledge the financial support from the National Natural Science Foundation of China (21788102), the Nation Key Basic Research and Development Program of China (973 program, 2015CB655004) Founded by MOST, the Guangdong Natural Science Funds for Distinguished Young Scholar (2014A030306035), the Science and Technology Program of Guangzhou (201804020027), and International Science and Technology Cooperation Program of Guangzhou (201704030069).

■ REFERENCES

(1) Grimsdale, A. C.; Leok Chan, K.; Martin, R. E.; Jokisz, P. G.; Holmes, A. B. Synthesis of Light-Emitting Conjugated Polymers for Applications in Electroluminescent Devices. *Chem. Rev.* **2009**, *109*, 897–1091.

DOI: 10.1021/acsami.9b03177
ACS Appl. Mater. Interfaces 2019, 11, 17592–17601

(2) Yang, X.; Zhou, G.; Wong, W.-Y. Functionalization of Phosphorescent Emitters and Their Host Materials by Main-Group Elements for Phosphorescent Organic Light-Emitting Devices. *Chem. Soc. Rev.* **2015**, *44*, 8484−8575.
(3) Zhao, Z.; Deng, C.; Chen, S.; Lam, J. W. Y.; Qin, W.; Lu, P.; Wang, Z.; Kwok, H. S.; Ma, Y.; Qiu, H.; Tang, B. Z. Full Emission Color Tuning in Luminogens Constructed from Tetraphenylethene, Benzo-2,1,3-thiadiazole and Thiophene Building Blocks. *Chem. Commun.* **2011**, *47*, 8847−8849.
(4) Uchida, M.; Izumizawa, T.; Nakano, T.; Yamaguchi, S.; Tamao, K.; Furukawa, K. Structural Optimization of 2,5-Diarylsiloles as Excellent Electron-Transporting Materials for Organic Electroluminescent Devices. *Chem. Mater.* **2001**, *13*, 2680−2683.
(5) Park, T. J.; Jeon, W. S.; Park, J. J.; Kim, S. Y.; Lee, Y. K.; Jang, J.; Kwon, J. H.; Pode, R. Efficient simple structure red phosphorescent organic light emitting devices with narrow band-gap fluorescent host. *Appl. Phys. Lett.* **2008**, *92*, 113308.
(6) Chien, C.-H.; Chen, C.-K.; Hsu, F.-M.; Shu, C.-F.; Chou, P.-T.; Lai, C.-H. Multifunctional Deep-Blue Emitter Comprising an Anthracene Core and Terminal Triphenylphosphine Oxide Groups. *Adv. Funct. Mater.* **2009**, *19*, 560−566.
(7) Xing, X.; Zhang, L.; Liu, R.; Li, S.; Qu, B.; Chen, Z.; Sun, W.; Xiao, L.; Gong, Q. A Deep-Blue Emitter with Electron Transporting Property to Improve Charge Balance for Organic Light-Emitting Device. *ACS Appl. Mater. Interfaces* **2012**, *4*, 2877−2880.
(8) Matthews, J. R.; Niu, W.; Tandia, A.; Wallace, A. L.; Hu, J.; Lee, W.-Y.; Giri, G.; Mannsfeld, S. C. B. Scalable Synthesis of Fused Thiophene-Diketopyrrolopyrrole Semiconducting Polymers Processed from Nonchlorinated Solvents into High Performance Thin Film Transistors. *Chem. Mater.* **2013**, *25*, 782−789.
(9) Yuan, Y.; Chen, J.-X.; Lu, F.; Tong, Q.-X.; Yang, Q.-D.; Mo, H.-W.; Ng, T.-W.; Wong, F.-L.; Guo, Z.-Q.; Ye, J.; Chen, Z.; Zhang, X.-H.; Lee, C.-S. Bipolar Phenanthroimidazole Derivatives Containing-Bulky Polyaromatic Hydrocarbons for Nondoped Blue Electroluminescence Devices with High Efficiency and Low Efficiency Roll-Off. *Chem. Mater.* **2013**, *25*, 4957−4965.
(10) Tang, X.; Bai, Q.; Shan, T.; Li, J.; Gao, Y.; Liu, F.; Liu, H.; Peng, Q.; Yang, B.; Li, F.; Lu, P. Efficient Nondoped Blue Fluorescent Organic Light-Emitting Diodes (OLEDs) with a High External Quantum Efficiency of 9.4% @ 1000 cd m^{-2} Based on Phenanthroimidazole−Anthracene Derivative. *Adv. Funct. Mater.* **2018**, *28*, 1705813.
(11) Huang, J.; Su, J.-H.; Li, X.; Lam, M.-K.; Fung, K.-M.; Fan, H.-H.; Cheah, K.-W.; Chen, C. H.; Tian, H. Bipolar Anthracene Derivatives Containing Hole- and Electron-Transporting Moieties for Highly Efficient Blue Electroluminescence Devices. *J. Mater. Chem.* **2011**, *21*, 2957−2964.
(12) Liu, B.; Nie, H.; Zhou, X.; Hu, S.; Luo, D.; Gao, D.; Zou, J.; Xu, M.; Wang, L.; Zhao, Z.; Qin, A.; Peng, J.; Ning, H.; Cao, Y.; Tang, B. Z. Manipulation of Charge and Exciton Distribution Based on Blue Aggregation-Induced Emission Fluorophors: A Novel Concept to Achieve High-Performance Hybrid White Organic Light-Emitting Diodes. *Adv. Funct. Mater.* **2016**, *26*, 776−783.
(13) Hu, J.-Y.; Pu, Y.-J.; Satoh, F.; Kawata, S.; Katagiri, H.; Sasabe, H.; Kido, J. Bisanthracene-Based Donor−Acceptor-Type Light-Emitting Dopants: Highly Efficient Deep-Blue Emission in Organic Light-Emitting Devices. *Adv. Funct. Mater.* **2014**, *24*, 2064−2071.
(14) Kim, R.; Lee, S.; Kim, K.-H.; Lee, Y.-J.; Kwon, S.-K.; Kim, J.-J.; Kim, Y.-H. Extremely Deep Blue and Highly Efficient Non-Doped Organic Light Emitting Diodes Using an Asymmetric Anthracene Derivative with A Xylene Unit. *Chem. Commun.* **2013**, *49*, 4664−4669.
(15) Fukagawa, H.; Shimizu, T.; Ohbe, N.; Tokito, S.; Tokumaru, K.; Fujikake, H. Anthracene Derivatives as Efficient Emitting Hosts for Blue Organic Light-Emitting Diodes Utilizing Triplet-Triplet Annihilation. *Org. Electron.* **2012**, *13*, 1197−1203.
(16) Xue, K.; Sheng, R.; Duan, Y.; Chen, P.; Chen, B.; Wang, X.; Duan, Y.; Zhao, Y. Efficient Non-Doped Monochrome and White Phosphorescent Organic Light-Emitting Diodes Based on Ultrathin Emissive Layers. *Org. Electron.* **2015**, *26*, 451−457.
(17) Xue, K.; Han, G.; Duan, Y.; Chen, P.; Yang, Y.; Yang, D.; Duan, Y.; Wang, X.; Zhao, Y. Doping-Free Orange and White Phosphorescent Organic Light-Emitting Diodes with Ultra-Simply Structure and Excellent Color Stability. *Org. Electron.* **2015**, *18*, 84−88.
(18) Yin, Y.; Yu, J.; Cao, H.; Zhang, L.; Sun, H.; Xie, W. Efficient Non-Doped Phosphorescent Orange, Blue and White Organic Light-Emitting Devices. *Sci. Rep.* **2015**, *4*, 6754.
(19) Xia, D.; Wang, B.; Chen, B.; Wang, S.; Zhang, B.; Ding, J.; Wang, L.; Jing, X.; Wang, F. Self-Host Blue-Emitting Iridium Dendrimer with Carbazole Dendrons: Nondoped Phosphorescent Organic Light-Emitting Diodes. *Angew. Chem., Int. Ed.* **2014**, *126*, 1066−1070.
(20) Zhao, Y.; Chen, J.; Ma, D. Ultrathin Nondoped Emissive Layers for Efficient and Simple Monochrome and White Organic Light-Emitting Diodes. *ACS Appl. Mater. Interfaces* **2013**, *5*, 965−971.
(21) Hu, R.; Lager, E.; Aguilar-Aguilar, A.; Liu, J.; Lam, J. W. Y.; Sung, H. H. Y.; Williams, I. D.; Zhong, Y.; Wong, K. S.; Peña-Cabrera, E.; Tang, B. Z. Twisted Intramolecular Charge Transfer and Aggregation-Induced Emission of BODIPY Derivatives. *J. Phys. Chem. C* **2009**, *113*, 15845−15853.
(22) Peng, Q.; Yi, Y.; Shuai, Z.; Shao, J. Toward Quantitative Prediction of Molecular Fluorescence Quantum Efficiency: Role of Duschinsky Rotation. *J. Am. Chem. Soc.* **2007**, *129*, 9333−9339.
(23) Peng, Q.; Yi, Y.; Shuai, Z.; Shao, J. Excited State Radiationless Decay Process with Duschinsky Rotation Effect: Formalism and Implementation. *J. Chem. Phys.* **2007**, *126*, 114302.
(24) Shi, H.; Xin, D.; Gu, X.; Zhang, P.; Peng, H.; Chen, S.; Lin, G.; Zhao, Z.; Tang, B. Z. The Synthesis of Novel AIE Emitters with The Triphenylethene-Carbazole Skeleton and Para-/Meta-Substituted Arylboron Groups and Their Application in Efficient Non-Doped OLEDs. *J. Mater. Chem. C* **2016**, *4*, 1228−1237.
(25) Chen, B.; Liu, B.; Zeng, J.; Nie, H.; Xiong, Y.; Zou, J.; Ning, H.; Wang, Z.; Zhao, Z.; Tang, B. Z. Efficient Bipolar Blue AIEgens for High-Performance Nondoped Blue OLEDs and Hybrid White OLEDs. *Adv. Funct. Mater.* **2018**, *28*, 1803369.
(26) Wu, C.; Wu, Z.; Wang, B.; Li, X.; Zhao, N.; Hu, J.; Ma, D.; Wang, Q. Versatile Donor-π-Acceptor-Type Aggregation-Enhanced Emission Active Fluorophores as Both Highly Efficient Nondoped Emitter and Excellent Host. *ACS Appl. Mater. Interfaces* **2017**, *9*, 32946−32956.
(27) Chen, L.; Jiang, Y.; Nie, H.; Hu, R.; Kwok, H. S.; Huang, F.; Qin, A.; Zhao, Z.; Tang, B. Z. Rational Design of Aggregation-Induced Emission Luminogen with Weak Electron Donor-Acceptor Interaction to Achieve Highly Efficient Undoped Bilayer OLEDs. *ACS Appl. Mater. Interfaces* **2014**, *6*, 17215−17225.
(28) Kim, J. Y.; Yasuda, T.; Yang, Y. S.; Adachi, C. Bifunctional Star-Burst Amorphous Molecular Materials for OLEDs: Achieving Highly Efficient Solid-State Luminescence and Carrier Transport Induced by Spontaneous Molecular Orientation. *Adv. Mater.* **2013**, *25*, 2666−2671.
(29) Du, X.; Qi, J.; Zhang, Z.; Ma, D.; Wang, Z. Y. Efficient Nondoped Near Infrared Organic Light-Emitting Devices Based on Fluorophores with Aggregation-Induced Emission Enhancement. *Chem. Mater.* **2012**, *24*, 2178−2185.
(30) Huang, J.; Sun, N.; Yang, J.; Tang, R.; Li, Q.; Ma, D.; Li, Z. Blue Aggregation-Induced Emission Luminogens: High External Quantum Efficiencies Up to 3.99% in LED Device, and Restriction of the Conjugation Length through Rational Molecular Design. *Adv. Funct. Mater.* **2014**, *24*, 7645−7654.
(31) Yuan, W. Z.; Chen, S.; Lam, J. W. Y.; Deng, C.; Lu, P.; Sung, H. H.-Y.; Williams, I. D.; Kwok, H. S.; Zhang, Y.; Tang, B. Z. Towards High Efficiency Solid Emitters with Aggregation-Induced Emission and Electron-Transport Characteristics. *Chem. Commun.* **2011**, *47*, 11216−11223.
(32) Bredas, J.-L. Mind the gap! *Mater. Horiz.* **2014**, *1*, 17−19.
(33) Tang, S.; Li, W.; Shen, F.; Liu, D.; Yang, B.; Ma, Y. Highly Efficient Deep-Blue Electroluminescence Based on The Triphenyl-

DOI: 10.1021/acsami.9b03177
ACS Appl. Mater. Interfaces 2019, 11, 17592−17601

amine Cored and Peripheral Blue Emitters with Segregative HOMO−LUMO Characteristics. *J. Mater. Chem.* **2012**, *22*, 4401−4408.
(34) Jung, J. W.; Jo, J. W.; Jung, E. H.; Jo, W. H. Recent Progress in High Efficiency Polymer Solar Cells by Rational Design and Energy Level Tuning of Low Bandgap Copolymers with Various Electron-Withdrawing Units. *Org. Electron.* **2016**, *31*, 149−170.
(35) Zhan, X.; Sun, N.; Wu, Z.; Tu, J.; Yuan, L.; Tang, X.; Xie, Y.; Peng, Q.; Dong, Y.; Li, Q.; Ma, D.; Li, Z. Polyphenylbenzene as a Platform for Deep-Blue OLEDs: Aggregation Enhanced Emission and High External Quantum Efficiency of 3.98%. *Chem. Mater.* **2015**, *27*, 1847−1854.
(36) Ding, L.; Sun, Y.-Q.; Chen, H.; Zu, F.-S.; Wang, Z.-K.; Liao, L.-S. A Novel Intermediate Connector with Improved Charge Generation and Separation for Large-Area Tandem White Organic Lighting Devices. *J. Mater. Chem. C* **2014**, *2*, 10403−10408.
(37) Chen, J.; Zhao, F.; Ma, D. Hybrid white OLEDs with fluorophors and phosphors. *Mater. Today* **2014**, *17*, 175−183.
(38) Su, S.-J.; Chiba, T.; Takeda, T.; Kido, J. Pyridine-Containing Triphenylbenzene Derivatives with High Electron Mobility for Highly Efficient Phosphorescent OLEDs. *Adv. Mater.* **2008**, *20*, 2125−2130.
(39) Xu, Z.; Gu, J.; Qiao, X.; Qin, A.; Tang, B. Z.; Ma, D. Highly Efficient Deep Blue Aggregation-Induced Emission Organic Molecule: A Promising Multifunctional Electroluminescence Material for Blue/Green/Orange/Red/White OLEDs with Superior Efficiency and Low Roll-Off. *ACS Photonics* **2019**, *6*, 767−778.
(40) Mayr, C.; Lee, S. Y.; Schmidt, T. D.; Yasuda, T.; Adachi, C.; Brütting, W. Efficiency Enhancement of Organic Light-Emitting Diodes Incorporating a Highly Oriented Thermally Activated Delayed Fluorescence Emitter. *Adv. Funct. Mater.* **2014**, *24*, 5232−5239.
(41) Yokoyama, D. Molecular Orientation in Small-Molecule Organic Light-Emitting Diodes. *J. Mater. Chem.* **2011**, *21*, 19187−19202.
(42) Sun, Y.; Giebink, N. C.; Kanno, H.; Ma, B.; Thompson, M. E.; Forrest, S. R. Management of Singlet and Triplet Excitons for Efficient White Organic Light-Emitting Devices. *Nature* **2006**, *440*, 908−912.
(43) Schwartz, G.; Pfeiffer, M.; Reineke, S.; Walzer, K.; Leo, K. Harvesting Triplet Excitons from Fluorescent Blue Emitters in White Organic Light-Emitting Diodes. *Adv. Mater.* **2007**, *19*, 3672−3676.
(44) Schwartz, G.; Reineke, S.; Rosenow, T. C.; Walzer, K.; Leo, K. Triplet Harvesting in Hybrid White Organic Light-Emitting Diodes. *Adv. Funct. Mater.* **2009**, *19*, 1319−1333.
(45) Ye, J.; Zheng, C.-J.; Ou, X.-M.; Zhang, X.-H.; Fung, M.-K.; Lee, C.-S. Management of Singlet and Triplet Excitons in a Single Emission Layer: A Simple Approach for a High-Efficiency Fluorescence/Phosphorescence Hybrid White Organic Light-Emitting Device. *Adv. Mater.* **2012**, *24*, 3410−3414.
(46) Kim, Y. J.; Son, Y. H.; Kwon, J. H. Highly Efficient Yellow Phosphorescent Organic Light-Emitting Diodes for Two-Peak Tandem White Organic Light-Emitting Diode Applications. *J. Inf. Disp.* **2013**, *14*, 109−113.
(47) Huang, W.-S.; Lin, J. T.; Chien, C.-H.; Tao, Y.-T.; Sun, S.-S.; Wen, Y.-S. Highly Phosphorescent Bis-Cyclometalated Iridium Complexes Containing Benzoimidazole-Based Ligands. *Chem. Mater.* **2004**, *16*, 2480−2488.
(48) Liu, B.; Li, X.-L.; Tao, H.; Zou, J.; Xu, M.; Wang, L.; Peng, J.; Cao, Y. Manipulation of Exciton Distribution for High-Performance Fluorescent/Phosphorescent Hybrid White Organic Light-Emitting Diodes. *J. Mater. Chem. C* **2017**, *5*, 7668−7683.
(49) Liu, B.-Q.; Wang, L.; Gao, D.; Zou, J.; Ning, H.; Peng, J.; Cao, Y. Extremely High-Efficiency and Ultrasimplified Hybrid White Organic Light-Emitting Diodes Exploiting Double Multifunctional Blue Emitting Layers. *Light: Sci. Appl.* **2016**, *5*, 16137−16142.
(50) Lee, J.; Chopra, N.; Eom, S.-H.; Zheng, Y.; Xue, J.; So, F.; Shi, J. Effects of Triplet Energies and Transporting Properties of Carrier Transporting Materials on Blue Phosphorescent Organic Light Emitting Devices. *Appl. Phys. Lett.* **2008**, *93*, 123306.
(51) Su, S.-J.; Chiba, T.; Takeda, T.; Kido, J. Pyridine-Containing Triphenylbenzene Derivatives with High Electron Mobility for Highly Efficient Phosphorescent OLEDs. *Adv. Mater.* **2008**, *20*, 2125−2130.
(52) Baldo, M. A.; O'Brien, D. F.; Thompson, M. E.; Forrest, S. R. Excitonic Singlet-Triplet Ratio in a Semiconducting Organic Thin Film. *Phys. Rev. B: Condens. Matter Mater. Phys.* **1999**, *60*, 14422.
(53) Rothberg, L. J.; Lovinger, A. J. Status of and Prospects for Organic Electroluminescence. *J. Mater. Res.* **1996**, *11*, 3174−3187.
(54) Sun, N.; Wang, Q.; Zhao, Y.; Chen, Y.; Yang, D.; Zhao, F.; Chen, J.; Ma, D. High-Performance Hybrid White Organic Light-Emitting Devices without Interlayer between Fluorescent and Phosphorescent Emissive Regions. *Adv. Mater.* **2014**, *26*, 1617−1621.
(55) Wang, J.; Chen, J.; Qiao, X.; Alshehri, S. M.; Ahamad, T.; Ma, D. Simple-Structured Phosphorescent Warm White Organic Light-Emitting Diodes with High Power Efficiency and Low Efficiency Roll-off. *ACS Appl. Mater. Interfaces* **2016**, *8*, 10093−10097.
(56) Zhuang, X.; Zhang, H.; Ye, K.; Liu, Y.; Wang, Y. Two Host−Dopant Emitting Systems Realizing Four-Color Emission: A Simple and Effective Strategy for Highly Efficient Warm-White Organic Light-Emitting Diodes with High Color-Rendering Index at High Luminance. *ACS Appl. Mater. Interfaces* **2016**, *8*, 11221−11225.
(57) Wu, Z.; Luo, J.; Sun, N.; Zhu, L.; Sun, H.; Yu, L.; Yang, D.; Yang, D.; Chen, J.; Qiao, X.; Chen, J.; Yang, C.; Ma, D. High-Performance Hybrid White Organic Light-Emitting Diodes with Superior Efficiency/Color Rendering Index/Color Stability and Low Efficiency Roll-Off Based on a Blue Thermally Activated Delayed Fluorescent Emitter. *Adv. Funct. Mater.* **2016**, *26*, 3306−3313.
(58) Gong, S.; Sun, N.; Luo, J.; Zhong, C.; Ma, D.; Qin, J.; Yang, C. Highly Efficient Simple-Structure Blue and All-Phosphor Warm-White Phosphorescent Organic Light-Emitting Diodes Enabled by Wide-Bandgap Tetraarylsilane-Based Functional Materials. *Adv. Funct. Mater.* **2014**, *24*, 5710−5718.
(59) Miao, Y.; Wang, K.; Zhao, B.; Gao, L.; Tao, P.; Liu, X.; Hao, Y.; Wang, H.; Xu, B.; Zhu, F. High-Efficiency/Cri/Color Stability Warm White Organic Light-Emitting Diodes by Incorporating Ultrathin Phosphorescence Layers in a Blue Fluorescence Layer. *Nanophotonics* **2018**, *7*, 295.
(60) Li, X.-L.; Ouyang, X.; Chen, D.; Cai, X.; Liu, M.; Ge, Z.; Cao, Y.; Su, S.-J. Highly Efficient Blue and Warm White Organic Light-Emitting Diodes with a Simplified Structure. *Nanotechnology* **2016**, *27*, 124001.

DOI: 10.1021/acsami.9b03177
ACS Appl. Mater. Interfaces 2019, 11, 17592−17601